

10. K. G. Balmain, M. Gossland, R. D. Reeves, W. G. Kuller, in proceedings of an *International Symposium on Spacecraft Materials in Space Environment*, Toulouse, France, 8 to 12 June 1982 (European Space Agency, Noordwijk, Netherlands, 1982), pp. 263–268.
11. O. Berolo, *ibid.*, pp. 1–10.
12. J. E. Nanevitz and R. C. Adamo, *Prog. Astronaut. Aeronaut.* 71, 252 (1980).
13. The trailing side of I_0 experiences a higher flux of low energy electrons and ions than the leading side; however, it is the more energetic particles that are relevant to surface discharges.
14. T. Gold, *Science* 206, 1071 (1979).
15. We thank J. Nanevitz for helpful discussions and the use of his laboratory at SRI International. We also thank K. Hewitt and J. Thayer for discussions and assistance with the experiments, S. Lee for the sulfur samples, and F. Herbert and S. Croft for discussions. A portion of this work was supported by the National Aeronautics and Space Administration and NSF at the Planetary Science Institute (PSI). PSI is a division of Science Applications International Corporation; this is PSI contribution 271.

3 April 1989; accepted 14 June 1989

Nonequilibrium Molecular Motion in a Hypersonic Shock Wave

G. PHAM-VAN-DIEP, D. ERWIN, E. P. MUNTZ*

Molecular velocities have been measured inside a hypersonic, normal shock wave, where the gas experiences rapid changes in its macroscopic properties. As first hypothesized by Mott-Smith, but never directly observed, the molecular velocity distribution exhibits a qualitatively bimodal character that is derived from the distribution functions on either side of the shock. Quantitatively correct forms of the molecular velocity distribution function in highly nonequilibrium flows can be calculated, by means of the Direct Simulation Monte Carlo technique.

THE MOTION OF MOLECULES IN SYSTEMS that are not in equilibrium has attracted attention since the formulation of the Boltzmann equation (1–3). A convenient place to find extremely nonequilibrium conditions is the interior of a normal shock wave in a gas, where the macroscopic properties of the gas change dramatically over a few molecular mean free paths (4). Within a shock an upstream equilibrium distribution moving at supersonic speeds makes a transition to a downstream, higher temperature equilibrium distribution drifting at subsonic speeds. For hypersonic shocks the wave's thickness, which is the characteristic distance required for the upstream to downstream transition, is typically about five times the molecular mean free path in the undisturbed flow upstream of the shock front. For flows produced in a wind tunnel with a constant total energy (constant stagnation temperature), the upstream static temperature decreases as the flow Mach number (M) increases; as a result, the random molecular motion of the upstream molecules occupies a progressively smaller volume of velocity space. The higher the value of M , the easier it is to observe details of the transition in the molecular motion as the gas adjusts between its upstream and downstream distributions.

Such velocity space simplification pro-

vides advantages analogous to the simplification of rotational and vibrational spectra achieved by flow cooling in expanding gas flows (5). In the experiments described here velocity space simplification was used to observe the extremely nonequilibrium molecular motion in a $M = 25$ helium shock wave. The flow's upstream static temperature was 1.5 K, and the downstream temperature was 280 K. A qualitatively bimodal molecular velocity distribution function was observed and compared in detail to predictions from both the Direct Simulation Monte Carlo (DSMC) technique developed by Bird (6) and the Mott-Smith assumption (7) of a simple weighted combination of upstream and downstream equilibrium distributions. Both Bird and K. Nanbu [see discussions in (3, 6)] have shown that the assumptions used in implementing the DSMC technique can be made consistent with the assumptions underlying the Boltzmann equation.

In addition to shock waves in low-density gases, shocks in liquids have been studied (3, 8, 9), both with the use of the Navier-Stokes equations and molecular dynamics calculations. Temperature, density, and velocity profiles in liquid argon appear to be described successfully by the Navier-Stokes equations for behind-the-shock pressures up to about 30 kbar, as inferred by comparisons to molecular dynamics calculations (8). For a pressure of 400 kbar, the molecular dynamics calculation gives a thicker shock than the Navier-Stokes equations. A similar behavior is found in gases for $M > 2$ when

DSMC calculations of shock thickness are compared to results from the Navier-Stokes equations. On the basis of a molecular dynamics calculation, the 400-kbar liquid argon shock exhibits a temperature overshoot of the streamwise component of the random molecular motion (8) that is qualitatively similar to shock waves in low-density gases. On the other hand, application of the Mott-Smith molecular velocity distribution to a 400-kbar liquid argon shock apparently gives results that do not compare well to the molecular dynamics calculation (8). For low-density gases the Mott-Smith distribution describes the molecular motion adequately at $M = 1.59$ (10) but not at $M = 25$. In the dilute gas limit, molecular dynamics calculations represent a solution of the Boltzmann equation but are computationally inefficient as compared to the DSMC technique (3, 6).

Measurements of the molecular velocity distribution functions in normal shock waves have been reported for $M = 1.59$ in helium (11) and $M = 7.18$ in argon (12). In each case the distribution functions were observed by measuring the intensity profiles of predominantly Doppler-broadened emission lines excited by an electron beam with a diameter of ~ 1 mm and an energy of 20 keV as it passed through the shock. Known as the electron beam fluorescence technique, it has been described in detail elsewhere (13). Electron beam fluorescence is useful in gases such as helium that cannot conveniently be probed by laser-induced fluorescence techniques. Emission from a short length (≈ 1 mm) of the stimulated radiation was used in the experiments. Spectral and thus, by means of the Doppler effect, velocity-

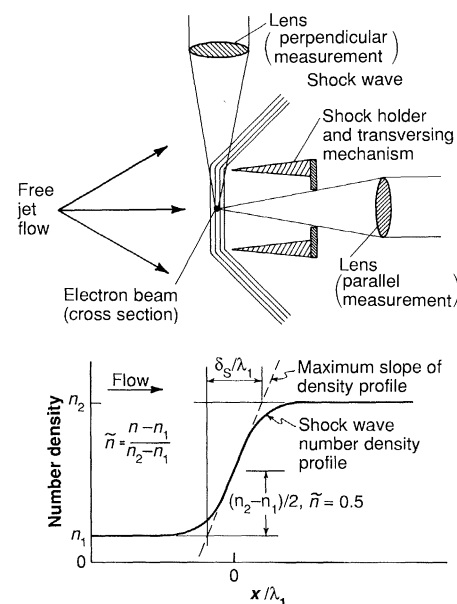


Fig. 1. Experimental arrangement and nomenclature; λ_1 , mean free path.

Department of Aerospace Engineering, University of Southern California, Los Angeles, CA 90089.

*To whom correspondence should be addressed.

space resolution was achieved with two Fabry-Perot etalons operated in tandem [see (12, 14) for details]. The combination of instrument, natural, and excitation broadening was small for the previous $M = 1.59$ helium measurements but quite significant compared to the Doppler broadening for the $M = 7.18$ argon results; a direct observation of the bimodal nature of the distribution function was not possible in either of these two experiments. In the experiments reported here the total of all broadening sources other than Doppler broadening was small, being equivalent to about 2 K. The combination of small broadening and extreme velocity space simplification made it possible to observe bimodal distributions directly.

The velocity distribution function measurements are actually a simple moment of the distribution function because the excitation by the electrons is broad-band and not sensitive to molecular velocities. Velocity resolution is obtained only in the direction of the optical axis of the detection system. In this case two directions were used, directly upstream (referred to here as a parallel measurement) and perpendicular to the flow (referred to as a perpendicular measurement). The molecular motion in directions normal to the direction of the detector's optical axis is not seen, and thus the measurement is of the simple moment $F(w) = \iint f(u, v, w) du dv$, where $f(u, v, w)$ is the molecular velocity distribution function; u , v , and w are the molecular velocity components; and w is in the direction of the observation.

The $M = 25$ shock wave was generated in a low-density wind tunnel facility located at the University of California, Berkeley. A sketch of the experimental arrangement along with some shock wave nomenclature is shown in Fig. 1. The experiments were done as a preliminary to the $M = 1.59$ helium measurements and other low M studies in argon-helium mixtures (14). In order to produce a $M = 25$ shock, it was convenient to expand helium in a free jet expansion through an orifice 3 mm in diameter from a stagnation pressure of 150 torr and a temperature of 296 K. Helium was used as the test gas because of its large Doppler effect and because it can be expanded in a free jet to very low temperatures without forming clusters. A tube 7.6 cm in diameter and 3.8 cm long with sharpened edges at the upstream end was used as a shock holder. Its leading edge was placed 7.6 cm downstream of the jet's orifice. A variable-resistance flow constriction at the downstream end of the shock holder was used to adjust the shock to be flat. The shock had a maximum slope thickness of about 6 mm (δ_s in Fig. 1). The $M = 25$ shock was

studied by traversing the entire jet flow and shock holder relative to the electron beam (Fig. 1). At several geometric positions in the shock, line profiles were obtained for observations both perpendicular and parallel to the flow direction. The 5015.67 Å helium line ($3^1P \rightarrow 2^1S$) was observed, and attention was paid to potential experimental pitfalls (13).

Because of the shock's thickness and the diverging nature of the free jet flow, it was impossible to identify, relative to any ideal, one-dimensional normal shock wave, exactly where a particular measurement was being made. This was so despite shock wave density profiles that were also obtained with the electron beam fluorescence technique (15). Because of this uncertainty, the subsequent low M helium and helium-argon measurements, as well as the $M = 7.18$ argon study, were done in very nearly parallel, nozzle-generated free stream flows.

Because of the difficulty encountered in interpreting the shock wave in the free jet flow, the data on the distribution functions in the high M helium shock were not published when they were obtained (December 1966). Recently, we have been doing detailed comparisons, based on different intermolecular force laws, between DSMC technique predictions of molecular velocity distribution functions in the $M = 1.59$ and $M = 7.18$ shock waves (16). During this study

we discovered what appeared to be a way to interpret the $M = 25$ results. It was realized that the form of the parallel distributions is extremely sensitive to position in the shock wave, where the position is indicated by the nondimensional density rise \bar{n} (for the definition of \bar{n} , see Fig. 1). Taking a cue from this observation, we calculated parallel and perpendicular distribution functions, F_p and F_\perp , for a $M = 25$ shock as a function of \bar{n} . We accomplished the calculations by using a DSMC technique code developed by Erwin and Pham-Van-Diep (16), derived from Bird's most recent shock wave program (17). These particular calculations were done for a Maitland-Smith intermolecular potential (18) with a distance parameter of 2.976 Å and a well depth of 10.9 K; differential scattering cross sections derived from the potential were used in the calculations. The predicted parallel distributions were compared to the data in an iterative process in order to find the \bar{n} from the prediction at which the best match was obtained with each measured F_p . We did the comparisons by convolving the predicted distributions with the known instrument and natural line-broadening profiles. The \bar{n} giving the best fit to a particular experimental F_p was assigned as the \bar{n} position in a corresponding ideal normal shock wave for the geometric position of the measurements.

The results of the matching procedure are shown for two of four available positions in Fig. 2 with both F_p and F_\perp included; the \bar{n} found for each measurement position is indicated. A shock wave density profile can be constructed on the basis of the \bar{n} values determined by the matching and the known location of each measurement. With the number density that the diverging free stream would have at the center of the experimental shock as the free stream density, a DSMC technique prediction of the shock's density profile is in excellent agreement with the derived experimental points, providing credibility for the somewhat arbitrary procedure outlined above. The experimental profiles can be compared to Mott-Smith profiles for \bar{n} positions found from the DSMC comparison. A typical comparison of a Mott-Smith and an experimental distribution is shown in Fig. 3, where each distribution has been normalized by its maximum value to illustrate the differences in shape.

For both F_p and F_\perp the molecular motion is highly nonequilibrium (Fig. 2). For the perpendicular distributions the uncollided free-stream remnant has a zero average drift velocity, as does the downstream portion of the distributions. In the parallel direction the two are separated by the change in flow velocity across the shock wave. The distribu-

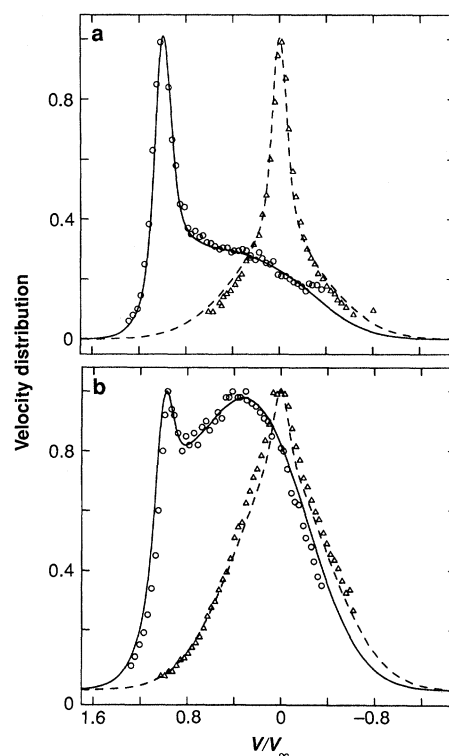


Fig. 2. Predicted and experimental velocity distributions: (a) $\bar{n} = 0.285$, (b) $\bar{n} = 0.565$; (Δ , \circ) experimental values; (—) DSMC parallel; (---) DSMC perpendicular.

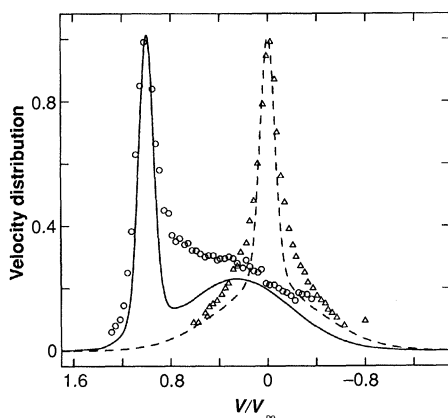


Fig. 3. Mott-Smith distribution and experiment ($\bar{n} = 0.285$), illustrating failure to account for scattered molecules. Refer to Fig. 2a for DSMC technique comparison to the same results.

tions in Fig. 2 exhibit qualitatively unmistakable bimodal forms that have not been observed directly in any other study. Such a form was originally hypothesized by Mott-Smith (7). The distributions predicted by the DSMC technique are quantitatively representative of the observed distributions. On the other hand, there is an obvious quantitative difference between the observations and the Mott-Smith distribution in Fig. 3, which is caused by the presence in the experimental results of a large population of scattered molecules with velocities intermediate between those of the upstream and those of the downstream equilibrium distributions. The comparison shown in Fig. 3 is typical of the quantitative relationship between the experiments and the Mott-Smith distributions for all of the positions in the shock for which data are available. Predictions of the shock wave distribution functions from numerical solutions of the Boltzmann equation due to Yen and Ng (19) also exhibit a bimodal structure that, although not directly comparable to the $M = 25$ results, appears qualitatively similar to the distributions measured in the experiments.

We believe that the distribution function measurements described here show that for monatomic gas flows with only elastic binary collisions, the DSMC technique provides an accurate quantitative prediction of the molecular motion in highly nonequilibrium gas flows. Because the scattered component of the molecular motion was particularly well isolated by the extreme simplification of the upstream distribution function, the quantitative agreement between experiment and prediction represents an important, detailed test of the prediction technique.

REFERENCES AND NOTES

1. S. Chapman, *Philos. Trans. R. Soc. London Ser. A* **216**, 279 (1916).

2. H. W. Liepmann, R. Narasimha, M. T. Chahine, *Phys. Fluids* **5** (no. 11), 1313 (1962).
3. D. J. Evans and W. G. Hoover, *Annu. Rev. Fluid Mech.* **18**, 243 (1986).
4. H. Alsmeyer, *J. Fluid Mech.* **74**, 497 (1976).
5. R. E. Smalley, L. Wharton, D. H. Levy, *J. Chem. Phys.* **63**, 4477 (1975).
6. G. A. Bird, *Annu. Rev. Fluid Mech.* **10**, 11 (1978).
7. H. M. Mott-Smith, *Phys. Rev.* **82**, 855 (1951).
8. B. L. Holian *et al.*, *Phys. Rev. A* **22**, 2793 (1980); B. L. Holian, *ibid.* **37**, 2562 (1988).
9. V. Yu. Klimenko and A. N. Dremin, *Sov. Phys. Dokl.* **24**, 984 (1980).
10. E. P. Muntz, *Annu. Rev. Fluid Mech.* **21**, 387 (1989).
11. _____ and L. M. Harnett, *Phys. Fluids* **12** (no. 10), 2027 (1969).
12. T. Holtz and E. P. Muntz, *ibid.* **26** (no. 9), 2425 (1983).
13. E. P. Muntz, *ibid.* **11** (no. 1), 64 (1968).
14. L. N. Harnett and E. P. Muntz, *ibid.* **15** (no. 4), 565 (1972).
15. E. P. Muntz, *The Electron Beam Fluorescence Technique* (Advisory Group for Aerospace Research and Development AGARDograph 132, Neuilly-sur-Seine, France, 1969 (copies available from Clearinghouse for Federal Scientific and Technical Information, Springfield, VA).
16. D. Erwin and G. Pham-Van-Diep, in *Rarefied Gas Dynamics*, E. P. Muntz, D. Campbell, D. Weaver, Eds. (American Institute of Aeronautics and Astronautics, Washington, DC, in press).
17. G. A. Bird, *ibid.*
18. G. C. Maitland, M. Rigby, E. B. Smith, W. A. Wakeham, *Intermolecular Forces* (Clarendon, Oxford, 1981).
19. S. M. Yen and W. Ng, *J. Fluid Mech.* **65**, 127 (1974).
20. The unpublished data reported here were obtained in December 1966 with the assistance of L. Harnett and A. Dichter. The cooperation of L. Talbot and his colleagues at the University of California, Berkeley, was essential. S. Abel and B. Miller reduced all of the data. J. F. Muntz set up a real-time data transmission system between Berkeley and Philadelphia and helped with the experiments. The experimental work was supported by the Air Force Office of Scientific Research, contract AF 49(638)1526. The more recent analysis was supported by a National Aeronautics and Space Administration-Department of Defense Hypersonic Training and Research grant, NASA NAGW-1061.

13 March 1989; accepted 9 June 1989

Synthesis of Organic Salts with Large Second-Order Optical Nonlinearities

SETH R. MARDER, JOSEPH W. PERRY, WILLIAM P. SCHAEFER

A series of organic salts, in which the cation has been designed to have a large molecular hyperpolarizability, has been prepared. Variation of the counterion (anion) in many cases leads to materials with large powder second harmonic generation efficiencies, the highest of which is roughly 1000 times that of a urea reference.

THE DESIRE TO UTILIZE NONLINEAR optical (NLO) properties of materials in applications such as telecommunications, optical data storage, and optical information processing has created a need for new materials with very large second-order susceptibilities [$\chi^{(2)}$] (1-3). It is well established that π donor-acceptor compounds with their large differences between ground-state and excited-state dipole moments as well as large transition dipole moments can exhibit large molecular second-order optical nonlinearities (4). It is imperative that the nonlinear molecules reside in a noncentrosymmetric environment if the molecular hyperpolarizability (β) is to lead to an observable bulk effect [$\chi^{(2)}$]. Roughly 75% of all organic molecules crystallize in centrosymmetric space groups, leading to materials with vanishing $\chi^{(2)}$ (5). Strategies used to overcome this major obstacle include the use of chiral molecules (6), the incorporation of functional groups that encourage asymmetric intermolecular hydrogen bonding (6, 7), the synthesis of molecules with very small ground-state dipole moments but larger excited-state dipole moments (8), and the incorporation of the chromophore into organic (9) and inorganic hosts (10). In addition to these approaches,

it is possible to orient the NLO active molecule in a glassy polymer matrix (11).

We present evidence that variation of counterions in organic salts is a simple and highly successful approach to creating materials with very large $\chi^{(2)}$. Meredith demonstrated that $(\text{CH}_3)_2\text{NC}_6\text{H}_4-\text{CH}=\text{CH}-\text{C}_5\text{H}_4\text{N}(\text{CH}_3)^+\text{CH}_3\text{SO}_4^-$ has a second harmonic generation (SHG) efficiency that is roughly 220 times that of urea (for a fundamental wavelength $\lambda = 1907$ nm) (12), which until recently (13) was the largest powder SHG efficiency reported. He suggested that in salts coulombic interactions could override the deleterious dipolar interactions that provide a strong driving force for centrosymmetric crystallization in covalent compounds (12). The use of ionic compounds further improves one's chances of achieving a noncentrosymmetric crystal structure because, in addition to the rationale described above, the counterions both separate and screen the dipolar chromophores from one another, thus reducing the

S. R. Marder and J. W. Perry, Jet Propulsion Laboratory, California Institute of Technology, Pasadena, CA 91109. W. P. Schaefer, Division of Chemistry and Chemical Engineering, California Institute of Technology, Pasadena, CA 91125.